J. Fluid Mech. (1985), *vol.* 154, *pp.* 121–144
Printed in Great Britain

Axisymmetric compressible flow in a rotating cylinder with axial convection

By MARIUS UNGARISH AND MOSHE ISRAELI
Computer Science Department, Technion – Israel Institute of Technology, Haifa, Israel

(Received 12 May 1983 and in revised form 27 April 1984)

The steady compressible flow of an ideal gas in a rotating annulus with thermally conducting walls is considered for small Rossby number ϵ and Ekman number E and moderate rotational Mach numbers M. Attention is focused on nonlinear effects which show up when σ and ϵM^2 are not small ($\sigma = \epsilon/HE^{\frac{1}{2}}$, H is the dimensionless height of the container). These effects are not properly predicted by the classical linear perturbation analysis, and are treated here by quasi-linear extensions.

The extra work required by these extensions is only the numerical solution of one ordinary differential equation for the pressure.

Numerical solutions of the full Navier–Stokes equations in the nonlinear range are presented, and the validity of the present approach is confirmed.

1. Introduction

In recent years there has been considerable interest in compressible flows in a rotating annulus. Valuable analytical results were obtained within the framework of a linear theory, i.e. the limit of infinitesimally small Rossby number ϵ. Sakurai & Matsuda (1974) and Matsuda, Sakurai & Takeda (1975) studied the steady-state flow in a container with perfectly conducting walls; the effects of insulated walls were considered by Matsuda & Hashimoto (1978) and Matsuda & Takeda (1978). Bark & Bark (1976) analysed the influence of the compressibility on the structure of the vertical Stewartson boundary layers. Spin-up and stability have been studied by Bark, Meijer & Cohen (1978) and Hultgren (1978). In a recent paper Conlisk, Foster & Walker (1982) analysed the flow field induced by sources and sinks on the vertical walls, differential rotation on the horizontal boundaries, and an axial applied thermal gradient.

The applicability of this theory is formally confined to a narrow range of parameters. The prominent restrictions are $\epsilon \ll HE^{\frac{1}{2}}$, imposed by neglecting the axial convection in the core, and $\epsilon \ll M^{-2}$, implied by linearization of the pressure term. (E is the Ekmann number, M the rotational Mach number and H the dimensionless length of the container.) The consequences of violating the abovementioned limits have not been emphasized in previous studies. Furthermore, verifications of theoretical predictions in the nonlinear range against experiments (almost unavailable) and numerical simulation are conspicuously lacking.

The task of the present work is twofold: (1) to emphasize certain nonlinearity effects and account for them in an extended asymptotic quasi-linear formulation; (2) to verify the asymptotic predictions by comparison with numerical solutions of the Navier–Stokes equations.

Before presenting the details, we outline several results. A more general formulation

of the perturbation equation for small ϵ has been obtained. This approach leads to one ordinary differential equation whose numerical solution, obtained by standard means and modest computer resources, provides the pressure, meridional velocities and density in the 'extended core' (inviscid regions + $E^{\frac{1}{4}}$ layers). This treatment overcomes the need of solving analytically the $E^{\frac{1}{4}}$ layers, which is a very difficult task when the density ρ varies in these layers, as typical of higher rotational Mach number. Moreover, since we use the local ρ (a consequence of perturbing $\ln P$ instead of P, where P is the pressure) and not the unperturbed solid-body density, our approach is free from the restriction $\epsilon M^2 \ll 1$. Subsequently, the elliptic temperature equation can be solved. It is shown that the decoupling between the pressure and temperature fields cannot be justified for long cylinders. The axial convection of temperature and azimuthal momentum (incorporated in our formulation to remove the restriction $\sigma = \epsilon/HE^{\frac{1}{2}} \ll 1$) does not influence the pressure field (to the leading order), but may affect considerably the temperature and the azimuthal velocity fields by increasing the influence of the Ekman layer on the boundary from which fluid is convected into the core. As convection dominates diffusion ($\sigma \to \infty$), the temperature and azimuthal velocity in the core are independent of z, their value is that of the 'edge' of the Ekman boundary layer, and matching the opposite Ekman layer requires an intermediate boundary layer of width $E^{\frac{1}{2}}/\epsilon$ where convection is balanced by diffusion. This feature (which was also mentioned by Conlisk *et al.* (1982) and resembles that of a Boussinesq fluid studied by Riley (1967) and Homsy & Hudson (1969)) has been confirmed by the numerical solutions of the Navier–Stokes equations.

In passing we note that the axial-convection terms may strongly affect the time-dependent development of the temperature and azimuthal velocity fields after the stage of spin-up (the $E^{-\frac{1}{2}}$ timescale). Thus, when $\epsilon/E^{\frac{1}{2}} > 1$, the dominant final adjustment of these fields may occur in a timescale $\epsilon^{-1}E^{-\frac{1}{2}}$ rather than E^{-1}.

The phenomenon of large perturbations in the pressure field arising from small perturbations of the velocity and temperature fields has also been verified by a numerical example, which, again, agrees well with our theory (i.e. the expansion of $\ln P$).

The good agreement between our solution of the approximate model and that of the full Navier–Stokes formulations gives credence to current theories about the behaviour of compressible rotating flows in the range of parameters under consideration.

2. Formulation

The objective is to describe the steady flow field of an ideal gas in a rotating annulus (figure 1), driven by imposed boundary conditions of velocity, stream function and temperature.

Let r_0^*, r_I^* and H^* be the outer and inner radii and height of the container (here the asterisk denotes dimensional variables). The mean temperature and angular velocity of the outer wall are Ω^* and T_0^*. The cylindrical system of coordinates (r, ϕ, z) rotates with Ω^* around the axis of symmetry z. If homogeneous boundary conditions are applied, a basic state of solid-body rotation is established and the resulting density at the outer wall is ρ_0^*, to be used subsequently as a reference quantity. The boundary conditions of interest, however, induce a motion of typical velocity $\epsilon\Omega^* r_0^*$.

Upon introducing the dimensionless length, velocity, temperature, density and pressure via the scaling

$$\{\boldsymbol{q}^*, T^*, \rho^*, P^*\} = \{(\epsilon\Omega^* r_0^*)\,\boldsymbol{q},\ T_0^*(1+\theta),\ \rho_0^*\,\rho,\ (\epsilon\Omega^{*2} r_0^{*2}\,\rho_0^*)\,P\},$$

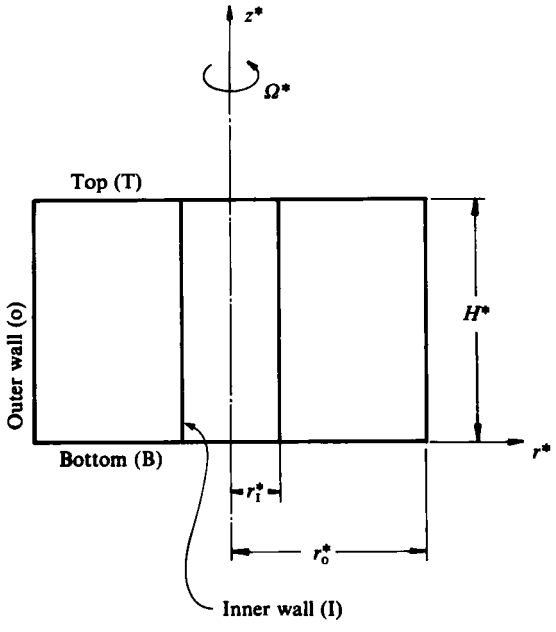

FIGURE 1. Description of the system.

the equations of motion (Greenspan 1969) can be expressed as follows:

continuity
$$\nabla\cdot\boldsymbol{q} = -uM^2r+\epsilon\left\{-u\frac{\partial\alpha}{\partial r}-w\frac{\partial\alpha}{\partial z}+(1+\epsilon\theta)^{-1}\left[u\frac{\partial\theta}{\partial r}+w\frac{\partial\theta}{\partial z}\right]\right\}; \tag{2.1}$$

radial momentum
$$\epsilon\left(\mathrm{D}u-\frac{v^2}{r}\right)-2v = -r\theta-\frac{1}{M^2}(1+\epsilon\theta)\frac{\partial\alpha}{\partial r}+\left(\frac{E}{\rho}\right)\left(\mathrm{L}u+\frac{1}{3}\frac{\partial}{\partial r}\nabla\cdot\boldsymbol{q}\right); \tag{2.2}$$

azimuthal momentum
$$\epsilon\left(\mathrm{D}v+\frac{uv}{r}\right)+2u = \frac{E}{\rho}\mathrm{L}v; \tag{2.3}$$

axial momentum
$$\epsilon\,\mathrm{D}w = -\frac{1}{M^2}(1+\epsilon\theta)\frac{\partial\alpha}{\partial z}+\frac{E}{\rho}\left(\nabla^2w+\frac{1}{3}\frac{\partial}{\partial z}\nabla\cdot\boldsymbol{q}\right); \tag{2.4}$$

energy
$$\epsilon\,Pr\,\mathrm{D}\theta-4b\left\{ur+\epsilon u\left[\theta r+\frac{1}{M^2}(1+\epsilon\theta)\frac{\partial\alpha}{\partial r}\right]+\epsilon w(1+\epsilon\theta)\frac{\partial\alpha}{\partial z}\right\} = \frac{E}{\rho}\nabla^2\theta+4b\epsilon\frac{E}{\rho}\Phi; \tag{2.5}$$

state
$$P = \frac{1}{\epsilon M^2}(1+\epsilon\theta)\rho; \tag{2.6}$$

where
$$\mathrm{D}\equiv u\frac{\partial}{\partial r}+w\frac{\partial}{\partial z},\quad \mathrm{L}\equiv\nabla^2-\frac{1}{r^2},$$
$$\nabla^2\equiv\frac{\partial^2}{\partial r^2}+\frac{1}{r}\frac{\partial}{\partial r}+\frac{\partial^2}{\partial z^2},$$
$$\boldsymbol{q}\equiv u\hat{\boldsymbol{r}}+v\hat{\boldsymbol{\phi}}+w\hat{\boldsymbol{z}}$$

and Φ is the dissipation function. The variable α, defined by

$$\nabla \ln P = M^2 r\hat{\mathbf{r}} + \epsilon \nabla \alpha, \tag{2.7}$$

and the equation of state (2.6) have been used to replace ∇P and $\nabla \rho$ in the foregoing equations.

The non-dimensional parameters are the Ekman number $E = \mu^*/\rho_0^* \Omega^* r_0^{*2}$, rotational isothermal Mach number $M = \Omega^* r_0^*/(R^* T_0^*)^{\frac{1}{2}}$, Brinkman number $b = 0.25\,\mu^* (\Omega^* r_0^*)^2/k^* T_0^*$ and Prandtl number, $Pr = \mu^* c_p^*/k$, where μ^*, R^*, k^* and c_p^* are respectively the viscosity, the gas constant, the coefficient of the thermal conductivity and the specific-heat coefficient at constant pressure. We assume that E is small, while Pr, M and b are of order unity. The (non-dimensional) height H of the cylinder is assumed to be large compared with the width of the horizontal Ekman layers (the opposite case is discussed by Israeli & Ungarish 1983). The effect of the gravity is neglected.

The introduction of α is motivated by the fact that the terms originally involving P and ρ become simple linear functions of α (with the exception of the coefficient of the viscous term), leading to subsequent simplifications. The physical interpretation of this variable becomes more evident from the integrated form of (2.7) and use of (2.6):

$$\rho = C\rho_{\mathrm{SB}}(r) \exp(\epsilon\alpha)(1+\epsilon\theta)^{-1}, \tag{2.8a}$$

$$P = CP_{\mathrm{SB}}(r) \exp(\epsilon\alpha), \tag{2.8b}$$

where C is a constant and the subscript SB denotes solid-body rotation, i.e.

$$\rho_{\mathrm{SB}}(r) = \exp(\tfrac{1}{2}M^2(r^2-1)), \tag{2.9a}$$

$$P_{\mathrm{SB}}(r) = (\epsilon M^2)^{-1} \rho_{\mathrm{SB}}(r). \tag{2.9b}$$

The next step is obtaining the equations of motion for small ϵ, attempting to circumvent possible restrictions imposed by non-uniform terms.

The classical linear theory considers infinitesimal ϵ. The corresponding equations are consequently obtained by substituting $\epsilon = 0$ in the system (2.1)–(2.5) with the subsidiary use of $\rho = \rho_{\mathrm{SB}}(r)$. Since from the standpoint of this approach $\exp(\epsilon\alpha) = 1+\epsilon\alpha$, the interpretation of α in the linear theory is simply

$$\epsilon\alpha = P/P_{\mathrm{SB}} - 1 \tag{2.10}$$

(see (2.8) and (2.9) with $C = 1$). The advantage of this approach lies in the possibility to proceed in the investigation by pure analytical means. On the other hand, the applicability of this theory to problems where ϵ is small but finite encounters strong limitations, and in particular $\epsilon/HE^{\frac{1}{2}} \ll 1$ and $\epsilon M^2 \ll 1$, as shown below.

The formulation employed in the present study abandons several analytical benefits of the linear theory for gaining an extension in the range of applicability. The resulting system, however, is amenable to straightforward numerical solution by standard methods (yielding great numerical accuracy by very modest computational resources).

In this formulation the genuine interpretation of α, including the term $\exp(\epsilon\alpha)$ in (2.8), is retained for the following reasons. Since $\alpha = O(M^2)$, as implied by (2.7), the perturbations of pressure and density are accordingly larger than those of velocity and temperature when M^2 is not small. This imposes the restriction $\epsilon M^2 \ll 1$ on using (2.10) instead of (2.8). This restriction of the linear theory obviously disappears when the linearized form (2.10) is not employed. (It can be shown that the present approach implies the formal expansion of $\ln P$ in powers of ϵ, while the linear theory uses a

similar expansion for P.) Note, however, that the term $\epsilon\theta$ in the right-hand side of (2.8a) can be neglected, to leading order, for calculating ρ.

A different type of restriction on ϵ is introduced because of the small E. The velocity components are of different orders of magnitude with respect to E, and thin boundary layers, implying steep derivatives, are present (e.g. in (2.1) ϵw may dominate u and $\epsilon\,\partial\theta/\partial r$ may be larger than 1). Unfortunately, if all the terms suspected of non-uniform behaviour are retained in (2.1)–(2.5), the remaining system is no more amenable to analysis than the original one, despite the small (but otherwise unrestricted) value of ϵ.

To proceed, the non-uniformity arising from small E is initially ignored, allowing for the cancellation of all the terms multiplied by ϵ in (2.1)–(2.5). This system is slightly different from the linear one (recall our treatment of the density) and is referred to thereafter as 'quasi-linear I'. The appropriate analysis is given in §3. Subsequently, the neglected terms are reconsidered, and the leading ones are also included in the 'quasi-linear II' system, resulting in an improved theory. Finally, a verification via comparison with numerical solution of the full Navier–Stokes equations is performed. The *ad hoc* formalism of the present approach is vindicated by the good agreement obtained in this verification.

The present approach requires an iterative solution of the equations, since α cannot be obtained separately. This, however, is easily performed on a computer. The boundary condition for α, reproduced by the constant C in (2.8), is specified by the amount of mass in the cylinder.

3. The quasi-linear I model

This approximation turns out to be a direct extension of the linear case, which has been studied by Sakurai & Matsuda (1974), Matsuda & Hashimoto (1978), Matsuda & Takeda (1978) and others. Initially, we recover previous results in a slightly more general way for several types of boundary conditions. Subsequently, we define an 'extended core' which includes the 'inviscid cores' and the outer Stewartson $E^{\frac{1}{4}}$ layers in the whole cylinder, and show that the pressure and velocity fields in this core can be obtained by solving a single ordinary differential equation and a single linear elliptic partial differential equation. Furthermore, we point out that the pressure and the temperature equations in this extended core are coupled unless $H \ll (E/\rho)^{-\frac{1}{2}}$. Finally, we briefly discuss the relative magnitude of the neglected nonlinear terms, in order to estimate the range of validity of this model.

3.1. *The horizontal Ekman layers*

The analysis of the flow in this layer is presented in Appendix A. The results that will be subsequently used are the matching conditions with the external 'core'.

Introducing the useful combination

$$\lambda = v - \tfrac{1}{2}r\theta, \tag{3.1}$$

denoting boundary conditions by capital letters, and using subscripts w for the wall and c for the core at the 'edge' of the Ekman layer, we obtain:

$$v_c = V_w + (\lambda_c - \lambda_w)\,(1+br^2)^{-1}, \tag{3.2}$$

$$\theta_c = \Theta_w - 2br(\lambda_c - \lambda_w)\,(1+br^2)^{-1}, \tag{3.3}$$

$$w_c = \frac{-1}{2} s \left(\frac{E}{\rho}\right)^{\frac{1}{2}} (1+br^2)^{-\frac{3}{4}} \left[\frac{1}{2r}(\lambda_c - \lambda_w)\left(-1+M^2r^2+\frac{3}{1+br^2}\right)+\frac{\mathrm{d}}{\mathrm{d}r}(\lambda_c-\lambda_w)\right]+W_w, \tag{3.4}$$

$$\tilde{\psi}_c = -\pi\rho r\left(\frac{E}{\rho}\right)^{\frac{1}{2}}(1+br^2)^{-\frac{3}{4}}(\lambda_c-\lambda_w), \tag{3.5}$$

where $\lambda_w = V_w - \frac{1}{2}\Theta_w$, $\tilde{\psi}_c$ is the mass flux transported by the Ekman layer, and $s = 1$ and -1 for the top and bottom plates. The value of λ_w is $O(1)$.

3.2. *The geostrophic balance*

Outside the Ekman layers we expect $\partial|q|/\partial z \sim H^{-1}|q|$ and $\partial|q|/\partial r = \delta_r^{-1}|q|$, where δ_r is the characteristic lengthscale in the radial direction ($\delta_r \sim 1$, $E^{\frac{1}{4}}H^{\frac{1}{2}}$ or $(EH)^{\frac{1}{3}}$).

From the equation of azimuthal momentum we obtain

$$u \sim \frac{E}{\rho}(\delta_r^{-2}+H^{-2})\,v. \tag{3.6}$$

Thus $|u| \ll |v|$ when $\delta_r, H \gg (E/\rho)^{\frac{1}{2}}$. Consequently, the viscous term of the radial momentum equation is negligibly small compared with the Coriolis term, and the radial momentum equation outside the Ekman boundary layers reduces to the geostrophic balance:

$$-2v+r\theta = -\frac{1}{M^2}\frac{\partial\alpha}{\partial r} \quad (=-2\lambda). \tag{3.7}$$

The axial changes of α are pronounced only in the $E^{\frac{1}{3}}$ vertical shear layers. In the main flow region (the 'extended core' defined in §3.4) each side of the geostrophic balance (3.7) is z-independent.

3.3. *The 'inviscid' core*

We consider the flow outside the Ekman layer, thus $\partial/\partial z = O(H^{-1})$, and assume $\partial/\partial r = O(1)$. Since the axial velocity induced by the Ekman layers is $O[(E/\rho)^{\frac{1}{2}}(1+M^2)\,v]$, the equation of axial momentum implies that the axial variation of $M^{-2}\alpha$ is much smaller than v. Consequently, the geostrophic radial balance (3.7) is of the form

$$-2v+r\theta = -\frac{1}{M^2}\frac{\mathrm{d}\alpha}{\mathrm{d}r} = -2\lambda(r). \tag{3.8}$$

Note that (3.8) and (2.8a) imply $\rho = \rho(r)$ to this order of approximation. In addition we use the azimuthal momentum and the energy equations:

$$2u = \frac{E}{\rho}\left(\nabla^2 v - \frac{v}{r^2}\right), \tag{3.9}$$

$$-4bru = \frac{E}{\rho}\nabla^2\theta. \tag{3.10}$$

Combination of (3.8)–(3.10) yields:

$$u = \frac{1}{2(1+br^2)}\frac{E}{\rho}\left[\frac{\mathrm{d}}{\mathrm{d}r}\frac{1}{r}\frac{\mathrm{d}}{\mathrm{d}r}r\lambda+\frac{\partial\theta}{\partial r}\right]. \tag{3.11}$$

Using the last two equations, we obtain

$$\frac{\partial^2\theta}{\partial r^2}+\frac{\partial^2\theta}{\partial z^2}+\frac{1+3br^2}{(1+br^2)r}\frac{\partial\theta}{\partial r}=\frac{-2br}{1+br^2}\frac{\mathrm{d}}{\mathrm{d}r}\frac{1}{r}\frac{\mathrm{d}}{\mathrm{d}r}r\lambda. \tag{3.12}$$

The boundary conditions for (3.12) on $z=0$, H provided by the value of θ at the edge of the Ekman boundary layer, are explicit functions of λ, cf. (3.3). Furthermore, (3.12) involves λ, and (as it will be shown) the corresponding boundary conditions on vertical walls are also related to λ. This points out the importance of λ for the solution of the flow field.

Computation of λ is possible via global mass continuity:

$$\Psi_{\mathrm{T}}-\Psi_{\mathrm{B}}=2\pi\int_0^H\rho r(\tilde{u}_{\mathrm{T}}+\tilde{u}_{\mathrm{B}}+u_{\mathrm{core}})\,\mathrm{d}z, \tag{3.13}$$

where Ψ_{T} and Ψ_{B} are the given boundary conditions on the stream function at the top and bottom disks respectively, $\tilde{u}_{\mathrm{T}}$ and $\tilde{u}_{\mathrm{B}}$ are the radial velocities in the Ekman boundary layers, and u_{core} is the radial velocity outside the Ekman layers, given by (3.11).

Integrating (3.11) and using the values of the stream-function correction in the Ekman layers, (3.5), we obtain

$$\begin{aligned}\Psi_{\mathrm{T}}-\Psi_{\mathrm{B}}=2\pi r\rho\left(\frac{E}{\rho}\right)^{\frac{1}{2}}\Big\{&[-\lambda+\tfrac{1}{2}(\lambda_{\mathrm{T}}+\lambda_{\mathrm{B}})](1+br^2)^{\frac{1}{4}}\\&+\frac{1}{2}\left(\frac{E}{\rho}\right)^{\frac{1}{2}}H\frac{\mathrm{d}}{\mathrm{d}r}\frac{1}{r}\frac{\mathrm{d}}{\mathrm{d}r}r\lambda+\frac{1}{2}\left(\frac{E}{\rho}\right)^{\frac{1}{2}}H\int_0^1\frac{\partial\theta}{\partial r}\mathrm{d}\left(\frac{z}{H}\right)\Big\}\frac{1}{1+br^2}.\end{aligned} \tag{3.14}$$

Recall that λ_{T} and λ_{B} are the prescribed values of $v-\frac{1}{2}r\theta$ on the top and bottom disks, of magnitude $O(1)$.

The last term in (3.14) couples the equation for λ to equation (3.12) for θ, unless the height $H\ll(E/\rho)^{-\frac{1}{2}}$. When $H\ll(E/\rho)^{-\frac{1}{2}}$ the second term in the right-hand side of (3.14) can also be ignored, resulting in

$$\lambda=\tfrac{1}{2}(\lambda_{\mathrm{T}}+\lambda_{\mathrm{B}})-\frac{\Psi_{\mathrm{T}}-\Psi_{\mathrm{B}}}{2\pi\rho(E/\rho)^{\frac{1}{2}}r}(1+br^2)^{\frac{1}{4}}. \tag{3.15}$$

In incompressible or in isothermal cases the coupling term does not appear (Moore & Saffman 1969; Toren & Solan 1979). In these cases $\lambda\equiv v$.

3.4. *The outer Stewartson $E^{\frac{1}{4}}$ shear layers and the extended core*

The term $\frac{1}{2}H(E/\rho)^{\frac{1}{2}}\mathrm{d}[r^{-1}\mathrm{d}(r\lambda)/\mathrm{d}r]/\mathrm{d}r$ which appears in (3.14) has been neglected in the 'inviscid core' where $\mathrm{d}/\mathrm{d}r=O(1)$. Consequently, λ in (3.15) has the same discontinuities as the symmetric component of the boundary conditions on the disks, namely $\lambda_{\mathrm{T}}+\lambda_{\mathrm{B}}$ and $\Psi_{\mathrm{T}}-\Psi_{\mathrm{B}}$ and does not take into account boundary conditions on the vertical walls or at the axis of rotation.

The term mentioned above is $O(1)$ in 'vertical' shear layers of radial width $\delta_r\sim H^{\frac{1}{2}}(E/\rho)^{\frac{1}{4}}$. The Ekman-layer adjustment for these vertical boundary layers yields, by (3.4), $w\sim(E/\rho)^{\frac{1}{4}}H^{-\frac{1}{2}}$. Inserting this value in the equation of axial momentum, we find that the axial changes of α are negligibly small; therefore the governing equations are again (3.8)–(3.10), and (3.11)–(3.14) are valid in the above vertical shear layers. Reconsidering the coupling term in (3.14) ($\partial\theta/\partial r$ is now $O[(E/\rho)^{-\frac{1}{4}}H^{-\frac{1}{2}}]$), we find that its order of magnitude is $[(E/\rho)^{\frac{1}{2}}H]^{\frac{1}{2}}$ and can be neglected for $H\ll(E/\rho)^{-\frac{1}{2}}$. In this

range the equation for λ can be solved separately. It is recalled that the same restriction on H allows us to ignore the coupling term in the inviscid core.

The equation for λ is now:

$$\frac{1}{2(1+br^2)^{\frac{1}{4}}}\left(\frac{E}{\rho}\right)^{\frac{1}{2}} H\frac{\mathrm{d}}{\mathrm{d}r}\left[\frac{1}{r}\frac{\mathrm{d}}{\mathrm{d}r}(r\lambda)\right]-\lambda = -\tfrac{1}{2}(\lambda_{\mathrm{T}}+\lambda_{\mathrm{B}})+\frac{\Psi_{\mathrm{T}}-\Psi_{\mathrm{B}}}{2\pi\rho(E/\rho)^{\frac{1}{2}}r}(1+br^2)^{\frac{3}{4}}. \tag{3.16}$$

Following Moore & Saffman (1969) and Toren (1976), we note that (3.16) is valid not only in the outer Stewartson layer, but also in the inner core (where the first term becomes negligibly small). The conclusion is that this equation defines an 'extended core' which covers, in fact, the whole flow field with the exception of the Ekman layer and the inner Stewartson layer. Accordingly, the boundary conditions for (3.16) must be given at $r = r_{\mathrm{I}}$ and $r = 1$. But on these boundaries λ $(= v-\frac{1}{2}r\theta)$ may be a prescribed function of the axial coordinate z, while (3.16) requires z-independent boundary values. Our expectation is that the appropriate boundary condition is the corresponding z-averaged value, and further analysis of the inner Stewartson layer (see §3.5) shows that this is indeed the case. Thus

$$\lambda(r = r_{\mathrm{b}}) = \frac{1}{H}\int_0^H (V_{\mathrm{b}}-\tfrac{1}{2}r_{\mathrm{b}}\Theta_{\mathrm{b}})\,\mathrm{d}z, \tag{3.17}$$

where $r_{\mathrm{b}} = r_{\mathrm{I}}$ or 1 and V_{b}, Θ_{b} are the boundary conditions for v and θ at these positions.

The temperature θ in this 'extended core' is given by the elliptic equation (3.12). The boundary condition on $z = 0$, H provided by the values of θ at the edge of the Ekman layers, (3.3), are explicit functions of λ. On the vertical boundaries $r = r_{\mathrm{I}}, 1$, θ matches the value at the edge of the inner thermal Stewartson layers (see §3.5), namely

$$\theta(r_{\mathrm{b}}, z) = \Theta_{\mathrm{b}}(z)+\frac{2br_{\mathrm{b}}}{1+br_{\mathrm{b}}^2}\left[(V_{\mathrm{b}}-\tfrac{1}{2}r_{\mathrm{b}}\Theta_{\mathrm{b}})-\frac{1}{H}\int_0^H (V_{\mathrm{b}}-\tfrac{1}{2}r_{\mathrm{b}}\Theta_{\mathrm{b}})\,\mathrm{d}z\right]. \tag{3.18}$$

In the case $r_{\mathrm{I}} = 0$ the appropriate boundary conditions are $\mathrm{d}\lambda/\mathrm{d}r = 0$ and $\partial\theta/\partial r = 0$.

After computing λ using (3.16) and θ, as described above, u can be obtained from (3.11) and v from $v = \lambda+\frac{1}{2}r\theta$. Thus the flow field in the 'extended core' is obtained by solving an ordinary differential equation of the second order for the pressure and an elliptic equation for the temperature. This formulation enables us to investigate the flow field induced by complicated boundary conditions in a compact and straightforward manner.

3.5. *The $E^{\frac{1}{3}}$ vertical shear layers*

In the 'extended core' the axial component $(\partial\alpha/\partial z)$ of the pressure gradient was neglected. Consequently this core cannot fulfil the imposed boundary condition on the vertical boundaries. Moreover, discontinuities in the horizontal boundary conditions give rise to 'jumps' in u and in w. In order to overcome these difficulties vertical shear layers of inner Stewartson type must be introduced into the solution of the extended core. The thickness of these layers is $O[(HE/\rho(r_{\mathrm{I}}))^{\frac{1}{3}}]$, where r_{I} denotes the radial position of the boundary layer. These regions are considered in Appendix B.

3.6. *The range of validity*

The order of magnitude of the flow-field variables resulting from the foregoing analysis is used to estimate the possible contribution of the discarded terms. The condition that these neglected terms remain relatively small leads to constraints of the form $\epsilon \ll f(E/\rho, H, b, M^2)$. If b and M are $O(1)$, we find the following restrictions.

1. *In the inviscid core*, $\epsilon \ll H(E/\rho)^{\frac{1}{2}}$. When ϵ approaches $H(E/\rho)^{\frac{1}{2}}$ from below, the axial convection terms $\epsilon\,\partial v/\partial z$ and $\epsilon\,\partial\theta/\partial z$ become pronounced in the equations of azimuthal momentum and of energy respectively. However, for the Ekman layers that connect the inviscid core to the horizontal boundaries the quasi-linear approach is uniformly valid. (In the homogeneous incompressible fluid and in the isothermal cases one obtains $\partial v/\partial z = 0$, the equations of momentum can be decoupled from the energy balance, and the present restriction does not show up.)

2. *In the $E^{\frac{1}{4}}$ Stewartson layers*, $\epsilon \ll H^{\frac{1}{2}}(E/\rho)^{\frac{1}{4}}$. The quasi-linear approach for the Ekman layers in this region is also restricted by this relation. A similar non-uniformity appears in the homogeneous incompressible fluid, and was studied by Barcilon (1970), Bennetts & Hocking (1973) and others. The present compressible problem is more complicated, because a large number of terms become involved as ϵ approaches $H^{\frac{1}{2}}(E/\rho)^{\frac{1}{4}}$.

3. *In the thermal $E^{\frac{1}{3}}$ layer*, $\epsilon \ll H^{\frac{1}{3}}(E/\rho)^{\frac{1}{3}}$. Most of the convection terms become pronounced as ϵ approaches $H^{\frac{1}{3}}(E/\rho)^{\frac{1}{3}}$. The same occurs in the respective Ekman layers.

4. *In the $E^{\frac{1}{3}}$ Stewartson layer*, $\epsilon \ll H^{\frac{2}{3}}(E/\rho)^{\frac{1}{3}}$. The behaviour is similar to that described in the above paragraph.

4. Inclusion of axial-convection terms in the quasi-linear II model

4.1. *The governing equations*

The foregoing considerations indicate that when $\sigma = \epsilon/HE^{\frac{1}{2}}$ is not small, the leading balance of momentum and energy in the 'inviscid core' is

$$-2v + r\theta = -\frac{1}{M^2}\frac{\partial \alpha}{\partial r}, \tag{4.1}$$

$$\epsilon w\frac{\partial v}{\partial z} + 2u = \frac{E}{\rho}\left(\nabla^2 v - \frac{v}{r^2}\right), \tag{4.2}$$

$$0 = -\frac{1}{M^2}\frac{\partial \alpha}{\partial z} + \frac{E}{\rho}\nabla^2 w, \tag{4.3}$$

$$\epsilon\, Pr\, w\frac{\partial \theta}{\partial z} - 4brw = \frac{E}{\rho}\nabla^2\theta. \tag{4.4}$$

Homsy & Hudson (1969) considered the thermal convection in a Boussinesq fluid ($b \to 0$) by including the first term in (4.4) but still neglecting the corresponding term in (4.2). This procedure implies the formal assumption that $Pr \gg 1$, which does not hold for gases. However, since the equation of azimuthal momentum was not explicitly used, the results presented there will not be affected by the neglected term even for $Pr = O(1)$. In the present case, owing to the compression work, the first term in (4.2) is quite important when $Pr \sim 1$.

An order-of-magnitude analysis of (4.3) shows that we can neglect the axial changes of α, obtaining for the radial equation (4.1):

$$-2v + r\theta = -2\lambda(r). \tag{4.5}$$

From (4.2), (4.4) and (4.5) we obtain

$$u = \frac{1}{2(1+br^2)}\left[\left(\frac{E}{\rho}\right)\left(\frac{\mathrm{d}}{\mathrm{d}r}\left[\frac{1}{r}\frac{\mathrm{d}}{\mathrm{d}r}(r\lambda)\right]+\frac{\partial\theta}{\partial r}\right)+\tfrac{1}{2}\epsilon wr(Pr-1)\frac{\partial\theta}{\partial z}\right]. \tag{4.6}$$

As expected, the last term in (4.6) is negligibly small when $\sigma \ll 1$. Apparently this term becomes dominant when σ increases, and $u = O(\epsilon E^{\frac{1}{2}})$ shows up in the core. But, as we shall show later, this is not the case, since $\partial\theta/\partial z$ tends to zero as σ becomes large. However, even for $u = O(\epsilon E^{\frac{1}{2}})$, the geostrophic balance (3.7) is valid.

Elimination of u from (4.4) and (4.6) gives for θ:

$$\frac{\partial^2\theta}{\partial r^2}+\frac{1+3br^2}{(1+br^2)\,r}\frac{\partial\theta}{\partial r}-\frac{\epsilon}{E/\rho}w\frac{Pr+br^2}{1+br^2}\frac{\partial\theta}{\partial z}+\frac{\partial^2\theta}{\partial z^2}=-\frac{2br}{1+br^2}\frac{\mathrm{d}}{\mathrm{d}r}\left[\frac{1}{r}\frac{\mathrm{d}(r\lambda)}{\mathrm{d}r}\right]. \tag{4.7}$$

As for the $\sigma = 0$ case, a single equation for λ can be obtained via the mass-continuity equation (3.13). The appropriate values of the integral in the Ekman boundary layer are given by (3.5). For u_{core} we use (4.6) to obtain

$$\begin{aligned}2\pi\rho\left(\frac{E}{\rho}\right)^{\frac{1}{2}} r\Bigg\{&\frac{1}{(1+br^2)^{\frac{3}{4}}}\left[-\lambda+\tfrac{1}{2}(\lambda_{\mathrm{T}}+\lambda_{\mathrm{B}})\right]\\ &+\frac{1}{2}\left(\frac{E}{\rho}\right)^{\frac{1}{2}}H\frac{1}{1+br^2}\frac{\mathrm{d}}{\mathrm{d}r}\left[\frac{1}{r}\frac{\mathrm{d}}{\mathrm{d}r}(r\lambda)\right]+\frac{1}{2}\left(\frac{E}{\rho}\right)^{\frac{1}{2}}H\frac{1}{1+br^2}\int_0^1\frac{\partial\theta}{\partial r}\mathrm{d}\left(\frac{z}{H}\right)\\ &+\tfrac{1}{4}\epsilon(Pr-1)\frac{1}{1+br^2}\int_0^H\frac{\partial\theta}{\partial z}w\left(\frac{E}{\rho}\right)^{-\frac{1}{2}}\mathrm{d}z\Bigg\}=\Psi_{\mathrm{T}}-\Psi_{\mathrm{B}}.\end{aligned} \tag{4.8}$$

The last term in the left-hand side is negligible compared with the first for $\epsilon \ll 1$, and the remaining equation is exactly (3.14). We may conclude that the axial convection in the inviscid core has only an $O(\epsilon)$ influence on the pressure gradient (reproduced by λ) independent of the value of σ.

Furthermore, we find that the equation for λ obtained for $\sigma \to 0$ in the extended core is also valid in the present case. The real restriction on this equation is imposed now by the non-uniformity in the $E^{\frac{1}{4}}$ Stewartson layer, which appears as ϵ approaches $H^{\frac{1}{2}}(E/\rho)^{\frac{1}{4}}$. On the other hand, equation (3.15) for λ in the inviscid core is valid for all $\epsilon \ll 1$.

Now we claim that equation (4.7) for θ is asymptotically valid in the extended core, for the following reasons. The validity of this equation in the inviscid core was explained above. In the $E^{\frac{1}{4}}$ shear layer $w \sim (E/\rho)^{\frac{1}{4}}H^{-\frac{1}{2}}$, $\partial^2\theta/\partial r^2 \sim (E/\rho)^{-\frac{1}{2}}H^{-1}$, and the relative contribution of the convection term is

$$\frac{\partial\theta}{\partial z}w\frac{\epsilon}{E/\rho}\Big/\frac{\partial^2\theta}{\partial r^2}\sim\epsilon\left(\frac{E}{\rho}\right)^{-\frac{1}{4}}H^{-\frac{1}{2}}. \tag{4.9}$$

Since the restriction of the present approach in the extended core is $\epsilon \ll H^{\frac{1}{2}}(E/\rho)^{\frac{1}{4}}$, the ratio (4.9) is small. Accordingly, (4.7) provides the extension of the temperature equation to the case $\epsilon \ll H^{\frac{1}{2}}(E/\rho)^{\frac{1}{4}}$, in conjunction with the equation (3.16) for λ. The boundary conditions for (4.7) are obtained via the $E^{\frac{1}{3}}$ thermal boundary layer (for which the linear approach is valid as $\epsilon \ll E^{\frac{1}{3}}$) and via the Ekman layers.

4.2. *The flow field for large σ*

It was shown above that the axial convection in the core has no influence on the pressure distribution λ and on the axial mass flux ρw. On the other hand, the

temperature field θ and the azimuthal velocity v are, as expected, strongly influenced by the axial convection as σ increases towards and above 1.

Consider the order of magnitude of the terms in the elliptic equation (4.7), for which Dirichlet boundary conditions are imposed. When σ is small the temperature field is dominated by conduction. As σ increases, the thermal properties on that boundary which ejects the axial flux are convected into the core and dominate the conduction from the other boundaries. (The case of symmetric horizontal boundary conditions, when no axial velocity is present, is eliminated from this discussion.)

When σ is large there is no term in (4.7) to balance the axial convection, therefore the leading balance of the temperature in the core yields:

$$\frac{\partial \theta}{\partial z} = 0 \quad \text{or} \quad \theta = \theta(r). \tag{4.10}$$

This solution can satisfy the boundary condition imposed by the horizontal plate from which mass is convected into the core, at $z = 0$, say. In order to match the boundary condition (3.3) on the edge of the Ekman boundary layer on the opposite plate, $z = H$, say, an additional horizontal boundary layer is required, where

$$-\frac{\epsilon}{(E/\rho)^{\frac{1}{2}}}\frac{w}{(E/\rho)^{\frac{1}{2}}}\frac{Pr+br^2}{1+br^2}\frac{\partial \theta}{\partial z}+\frac{\partial^2 \theta}{\partial z^2} = 0. \tag{4.11}$$

We assumed that $w > 0$, therefore (4.11) describes a boundary layer of thickness $O[(E/\rho)^{\frac{1}{2}}/\epsilon]$, where the Ekman region is a thin sublayer. Matching the solution of (4.10) and (4.11) to the boundary condition at the edge of the Ekman layer, we obtain

$$\left.\begin{aligned} \theta &= \theta(z=0)+A\,\mathrm{e}^{-\beta(H-z)}, \\ A &= \theta(z=H)-\theta(z=0), \\ \beta &= \frac{\epsilon}{(E/\rho)^{\frac{1}{2}}}\frac{w}{(E/\rho)^{\frac{1}{2}}}\frac{Pr+br^2}{1+br^2}. \end{aligned}\right\} \tag{4.12}$$

Here $\theta(z = 0)$ and $\theta(z = H)$ are the values at the edge of the lower and upper Ekman boundary layers, given by (3.3). A similar result was presented by Conlisk *et al.* (1982) for a particular case. This type of horizontal thermal boundary layer in stratified or slightly compressible fluid unbounded radially was also investigated by Duncan (1966), Riley (1967) and Hudson (1968*a*, *b*). Barcilon & Pedlosky (1967) showed that such a temperature distribution is incompatible with the boundary conditions on insulated vertical walls, and Homsy & Hudson (1969) matched it to thermally conducting vertical walls.

5. Numerical results

5.1. *Example 1*

A numerical experiment was made in order to verify the predicted features of the flow field for $\sigma \gg 1$. The system is presented in figure 2(*a*). The flow is induced by antisymmetric thermal perturbations $|\epsilon\theta| = 0.2$ on the horizontal walls, while the outer wall is held at a constant (zero) temperature. The solid boundaries are stationary with respect to the rotating frame. The isothermal rotational Mach number at the outer boundary is $M = 2\sqrt{1.4}$, and the Ekman number based on the maximal density is $E = 10^{-4}$. Other constants of the flow are $\gamma = 1.4$, $Pr = 0.70$. The numerical steady-state solution of the full Navier–Stokes equation was obtained by a finite-

difference time-marching scheme which conserves mass, momentum and total energy, similar to that used by Toren & Solan (1979). A staggered, stretched mesh was used, having 15 and 10 intervals in the radial and axial directions respectively.

Numerical results are presented in figure 2, and compared with approximate results obtained from the asymptotic approach. The representative value of ϵ is 0.2 (taking $|\theta| = 1$ on the horizontal boundaries), therefore $\sigma = \epsilon/E^{\frac{1}{2}}H = 20$, and we expect to find a pronounced influence of the thermal convection on the temperature and azimuthal velocity fields.

The stream function $\psi(= 2\pi \int_0^z \rho r u \, dz)$ is given in figure 2(*b*). The horizontal Ekman layers and the vertical $E^{\frac{1}{3}}$ boundary layer are clearly observed. In the core we find $2\pi\rho ur = \partial\psi/\partial z \approx 0$, as expected from (3.15) and (3.11) (here $\lambda_T + \lambda_B = 0$), while $\psi \sim E^{\frac{1}{2}}$ (owing to (3.5)). The radial distance between the streamlines increases towards the axis, since $\psi \sim \rho r^2$. No influence of the convection on ψ is observed.

The temperature and azimuthal velocity fields are non-symmetrical with respect to the midplane $z = \frac{1}{2}$. For example, the isotherms shown in figure 2(*c*) tend to concentrate near the lower plate, forming a thermal boundary-layer region of typical thickness 0.15, as a consequence of the axial thermal convection. More details are given in figures 2(*d*, *e*, *f*), which show profiles of θ, v/r and w as functions of z at certain radial positions; the first two are located in the inner core and the third in the $E^{\frac{1}{4}}$ region of the extended core. The asymptotic solution (dashed lines) is in good agreement with the numerical results (discrepancies of less than 15 % were obtained, which can be expected for $\epsilon = 0.2$). We recall that the classical linear theory predicts linear axial variations of v and θ in the core.

We see (figure 2*f*) that w in the core increases slightly with z. This results from

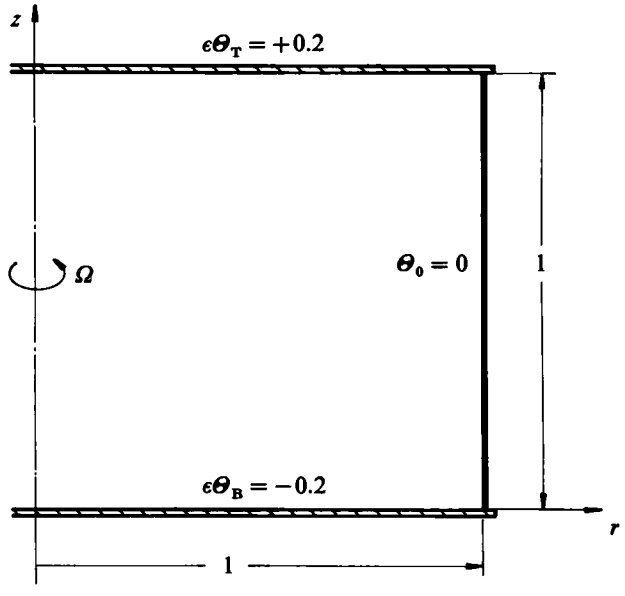

$V_w = 0 \quad E = 10^{-4} \quad M = 2\sqrt{1.4}$

(*a*)

FIGURE 2 (*a*). For caption see p. 136.

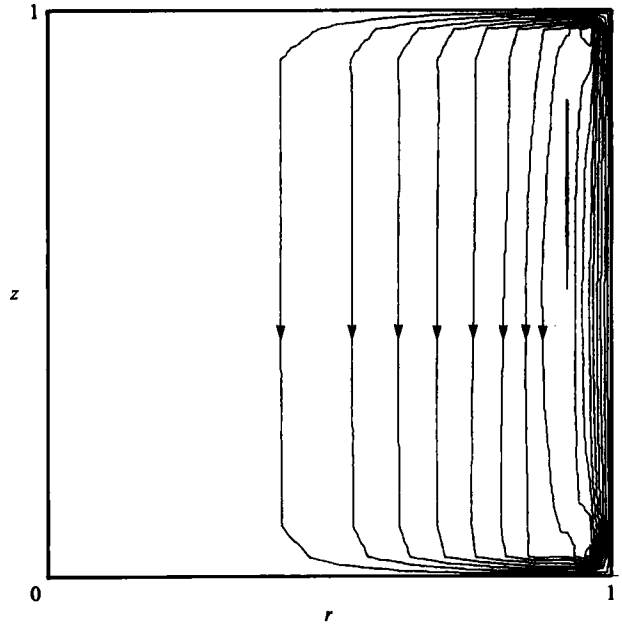

(*b*)

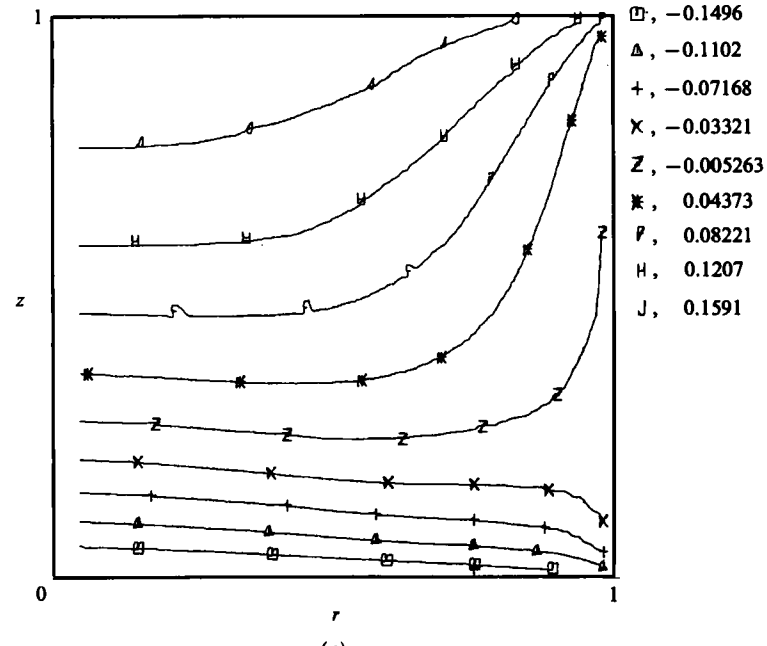

(*c*)

FIGURE 2 (*b*, *c*). For caption see p. 136.

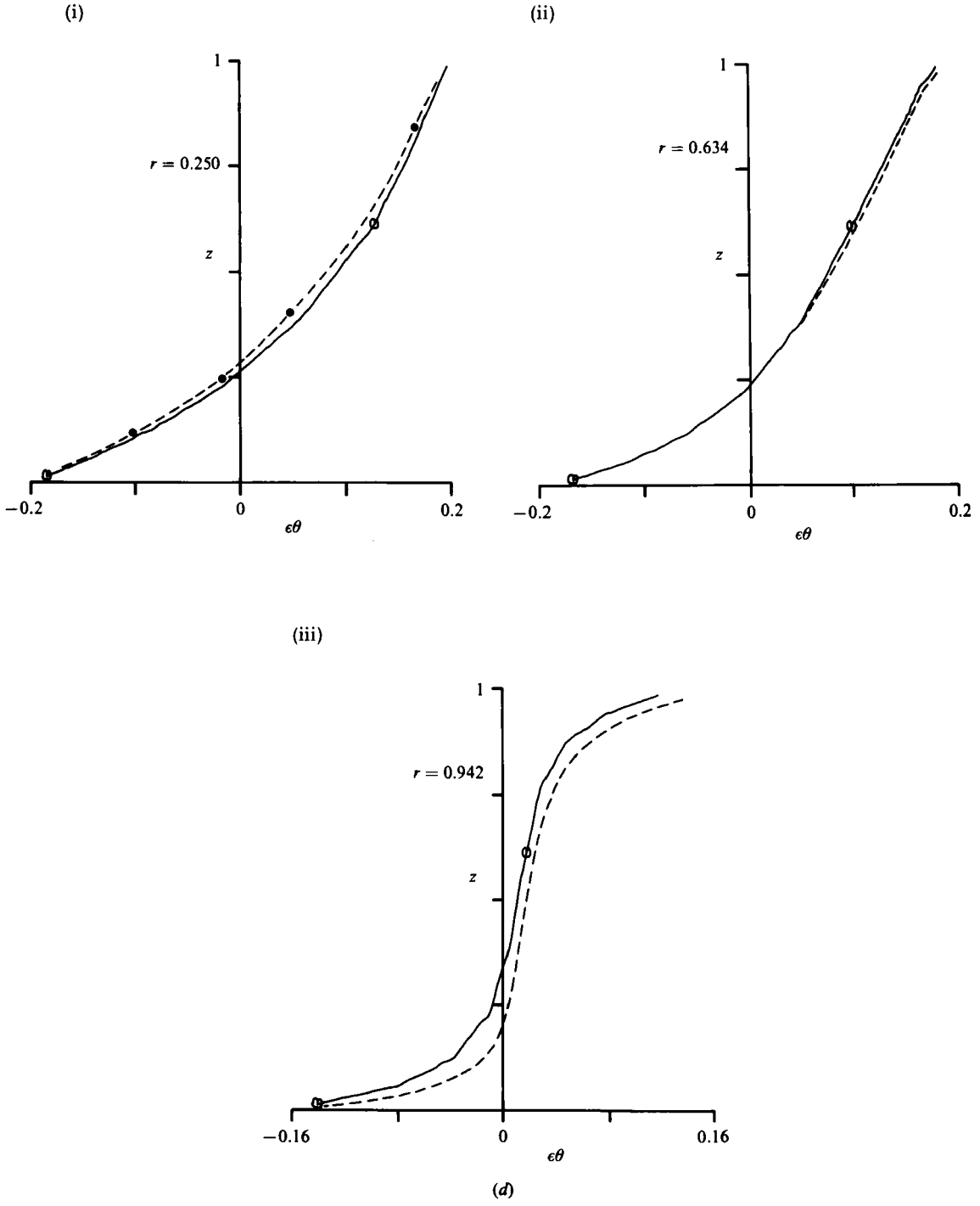

FIGURE 2 (*d*). For caption see p. 136.

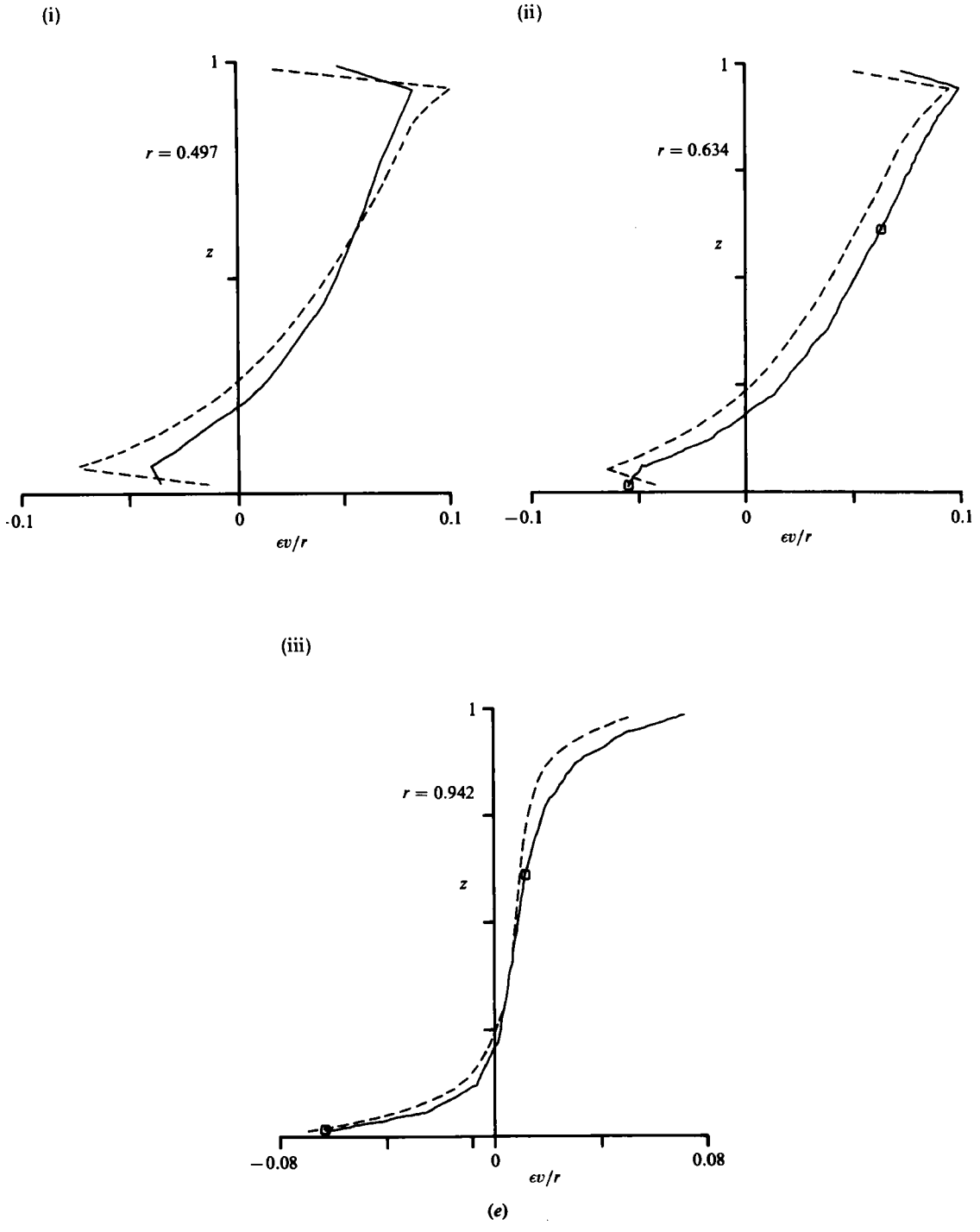

(*e*)

FIGURE 2 (*e*). For caption see p. 136.

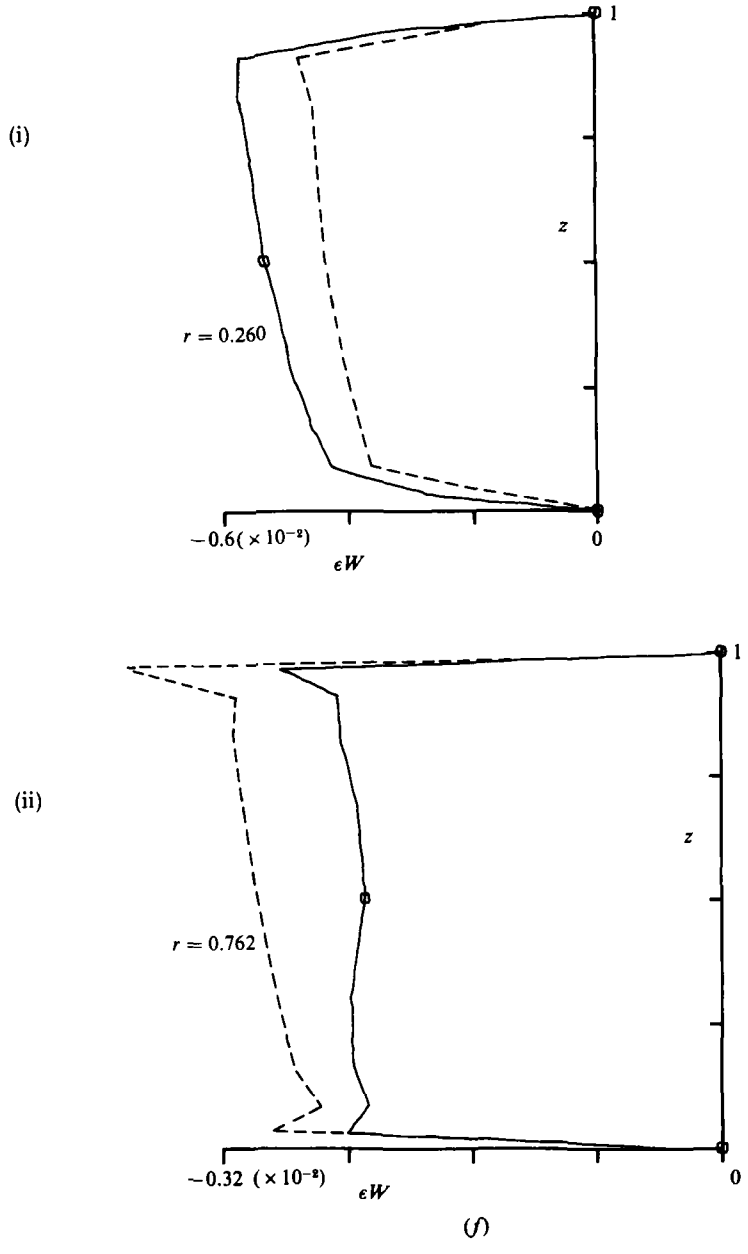

FIGURE 2. Example I: (*a*) boundary conditions; (*b*) stream function, $10^4 \epsilon\psi = 2.02\,(2.02)\,18.8$, numerical solution; (*c*) isotherms $\epsilon\theta$, numerical solution; (*d*) temperature profiles at constant radial position; (*e*) angular-velocity profiles at constant radial position; (*f*) axial-velocity profiles at constant radial position. (——, Numerical solution; – – –, approximate solution.)

the temperature distribution, which causes ρ to decrease with z. But the axial mass flux ρw is constant with z. We found that this feature of w can be reproduced by the asymptotic analysis by calculating ρw at the edge of the Ekman layers instead of w. The asymptotic prediction for w is less accurate than that for v or θ, since w, being $O(E^{\frac{1}{2}})$, is quite small in the interior.

5.2. *Example 2*

In the previous example the flow was induced by antisymmetric boundary conditions; therefore the perturbation of the pressure gradient λ was zero (to the leading order), according to (3.15). In the present example (figure 3*a*) we consider the flow induced by the bottom disk, which rotates 20% slower than the other walls; the theory predicts a 10% velocity perturbation in the interior, so that the effective Rossby number is $\epsilon = 0.1$. Thus the right-hand term in (3.15) is not zero, and a perturbation of the radial pressure gradient is expected. The Ekman number is $E = 2 \times 10^{-4}$, the rotational isothermal Mach number is $M = 2\sqrt{1.4}$, the Prandtl number is $Pr = 0.70$ and $\gamma = 1.4$.

The relative perturbation of the pressure is shown in figure 3(*b*). This perturbation reaches a value of about 35%, which is about $\frac{1}{2}M^2$ times larger than the perturbation of the angular velocity. The approximate solution, obtained by the expansion of $\ln P$ in powers of ϵ, is in excellent agreement with the numerical computation. Accordingly, the meridional flow, computed directly from the solution of the pressure (in fact, of λ) is also in good agreement, as shown in figures 3(*c*, *d*).

Good agreement was obtained also for the angular velocity (not shown here).

6. Discussion

An approximate analysis of the steady rotating compressible flow in a thermally conducting cylinder is performed and verified by numerical solutions.

The present model efficiently relaxes the most severe restrictions of classical linear theory, namely $\epsilon M^2 \ll 1$ and $\sigma \ll 1$. The first restriction is removed by employing the perturbation of $\nabla \ln P$ (reproduced by the variable α) and retaining the perturbed density ρ instead of the approximation ρ_{SB} in the equations. The latter restriction is treated by incorporating the axial-convection terms in the model.

This extension of the range of validity for quite general boundary conditions is achieved for the additional price of numerically solving one ordinary differential equation for the pressure. The solution is obtained in the 'extended core', which unifies the inviscid regions and the $E^{\frac{1}{4}}$ shear layers under equations valid in the continuous domain from boundary to boundary. Note that the present method of solution may be more efficient than the classical linear analytical method even in the range where the latter is applicable, especially when ρ varies considerably in the $E^{\frac{1}{4}}$ layers.

The predictions of the present model have been compared with numerical solutions of the full Navier–Stokes equations in the non-trivial range $\epsilon \sim 0.1$, $\sigma \sim 20$ and $\epsilon M^2 \sim 0.5$. The good agreement obtained in these comparisons justifies the somewhat *ad hoc* formalism of the present approach and strengthens the confidence in the applicability of perturbation theories to the problem under investigation. In particular, it is shown that the axial-convection terms, which become pronounced when σ is not small, do not affect the pressure and the axial-velocity field equations (obtained for $\sigma = 0$), but have a considerable influence on the temperature and azimuthal velocity fields.

The present approach is limited by the non-uniformity of the convection terms in the inner and outer Stewartson layers, namely $\epsilon \ll H^{\frac{1}{3}}(E/\rho)^{\frac{1}{3}}$ and $\epsilon \ll H^{\frac{1}{2}}(E/\rho)^{\frac{1}{4}}$. The extension of the asymptotic theory beyond these limits is apparently an extremely difficult task because of the large number of nonlinear terms that are involved. The

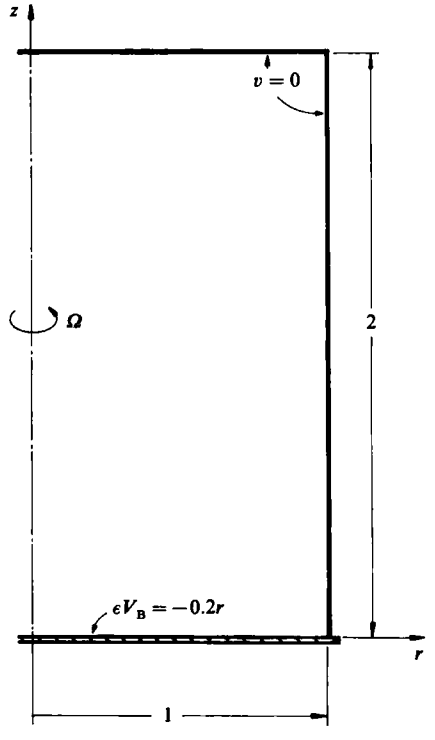

$\Theta_w = 0 \quad E = 2 \times 10^{-4} \quad M = 2\sqrt{1.4}$

(a)

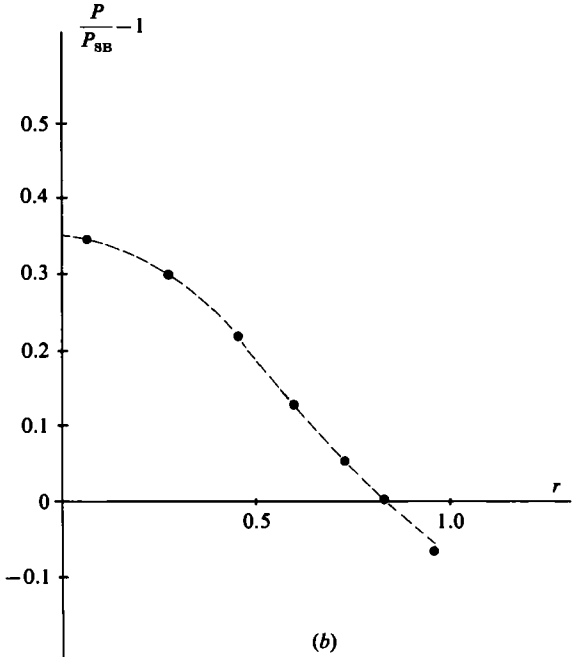

(b)

FIGURE 3 (a, b). For caption see facing page.

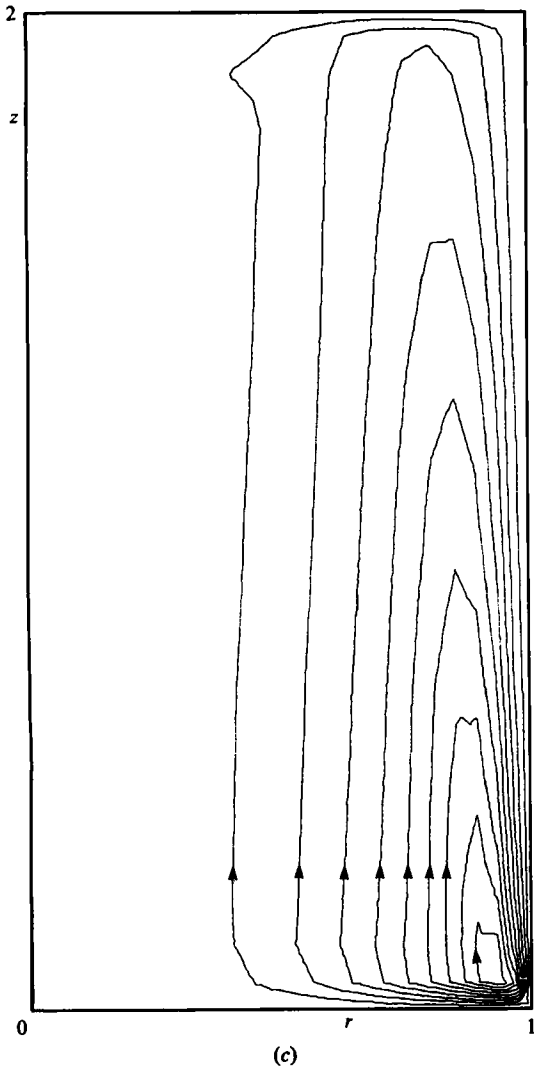

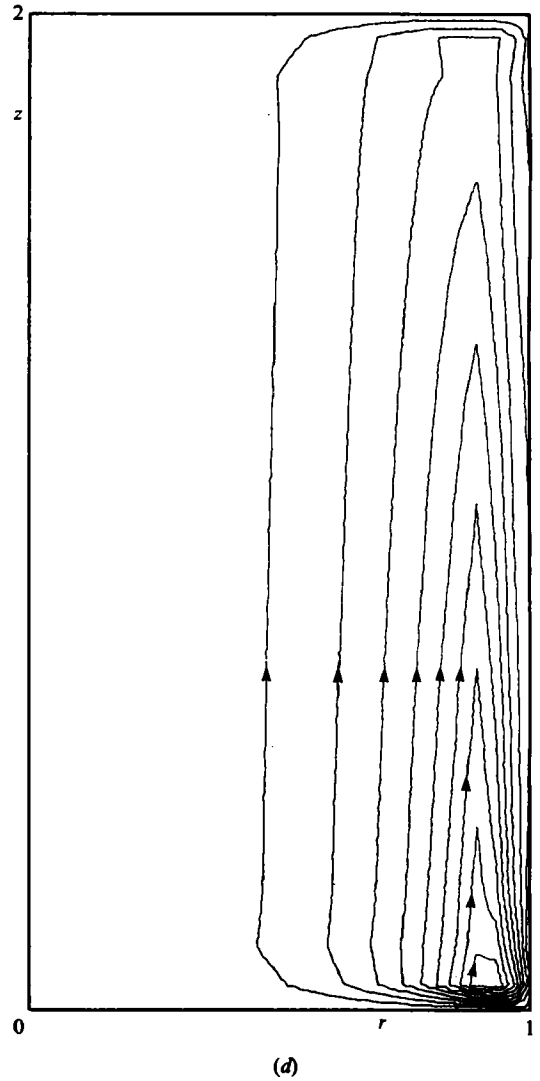

FIGURE 3. Example II: (*a*) boundary conditions; (*b*) $(P/P_{SB})-1$ at $z=1$, where P is the pressure and SB denotes solid-body rotation (●, numerical solution; ---, approximate solution); (*c*) stream function, $-10^4\epsilon\psi = 3.49\,(3.49)\,31.4$, numerical solution; (*d*) stream function, $-10^4\epsilon\psi = 3.72\,(3.72)\,33.48$, approximate solution.

investigation of this range calls for numerical solutions, for which the present approach can be used as a starting condition and as a basis for an improved-accuracy numerical scheme (Israeli & Ungarish 1981).

We would like to thank Professors A. Solan, M. Toren and H. P. Greenspan for very helpful discussions.

Appendix A. The horizontal Ekman layers

We denote by tildes the boundary-layer 'corrections' near the horizontal boundaries of the cylinder; thus

$$\{u, v, w, \theta, \alpha\} = \{u_c + \tilde{u}, v_c + \tilde{v}, w_c + \tilde{w}, \theta_c + \tilde{\theta}, \alpha_c + \tilde{\alpha}\}$$

where $(\ )_c$ is the value of the variable at the edge of the boundary layer. We assume that $(\tilde{\ })$ vary on an axial scale δ_z (which turns out to be $\sim (E/\rho)^{\frac{1}{2}}$), while the radial scale is δ_r, such that $\delta_z \ll \delta_r$.

The corresponding equations of motion are:

$$\frac{1}{r}\frac{\partial}{\partial r} r\tilde{u} + M^2 r\tilde{u} + \frac{\partial \tilde{w}}{\partial z} = 0, \tag{A 1}$$

$$-2\tilde{v} + r\tilde{\theta} = -\frac{1}{M^2}\frac{\partial \tilde{\alpha}}{\partial r} + \frac{E}{\rho}\frac{\partial^2 \tilde{u}}{\partial z^2}, \tag{A 2}$$

$$2\tilde{u} = \frac{E}{\rho}\frac{\partial^2 \tilde{v}}{\partial z^2}, \tag{A 3}$$

$$0 = -\frac{1}{M^2}\frac{\partial \tilde{\alpha}}{\partial z} + \frac{E}{\rho}\left(\frac{\partial^2 \tilde{w}}{\partial z^2} - \tfrac{1}{3}M^2 r\frac{\partial \tilde{u}}{\partial z}\right), \tag{A 4}$$

$$-4br\tilde{u} = \frac{E}{\rho}\frac{\partial^2 \tilde{\theta}}{\partial z^2}. \tag{A 5}$$

Let us consider the 'bottom' boundary, $z = 0$. The same analysis can be repeated for the top boundary. The boundary conditions for these equations are

$$\{\tilde{u}, \tilde{v}, \tilde{w}, \tilde{\theta}, \tilde{\alpha}\} \to 0 \quad \text{as } z \to \infty, \tag{A 6a}$$

$$\{\tilde{u}, \tilde{v}, \tilde{w}, \tilde{\theta}\} = \{-u_c, V_B - v_c, W_B - w_c, \Theta_B - \theta_c\} \quad \text{at } z = 0. \tag{A 6b}$$

Here V_B, W_B and Θ_B are the (specified) values on the bottom boundary. No-slip and perfect thermal conductivity at the solid surface were assumed.

We note that (A 3), (A 5) and the boundary condition at $z \to \infty$ imply the following relation:

$$\frac{\tilde{\theta}}{\tilde{v}} = -2br. \tag{A 7}$$

(It is worthwhile to mention that a similar relation also holds for the correction variables of the vertical boundary layers.)

Integrating (A 4) from z to ∞, anticipating $\rho = \rho(r)$ and using (A 1), we find

$$\frac{1}{M^2}\tilde{\alpha} = -\frac{E}{\rho}\left(\tfrac{4}{3}M^2 r\tilde{u} + \frac{1}{r}\frac{\partial}{\partial r} r\tilde{u}\right).$$

Therefore the first term in the right-hand side of (A 2) can be neglected in comparison with the second term, leading to the well-known result that the pressure in the boundary layer is induced by the outer core.

Now a single equation for $\tilde{u}$ can be obtained from (A 2), (A 7) and (A 3), namely

$$\frac{\partial^4 \tilde{u}}{\partial \zeta^4} + 4\tilde{u} = 0, \tag{A 8}$$

where ζ is the boundary-layer stretched coordinate:

$$\zeta = (E/\rho)^{-\frac{1}{2}}(1+br^2)^{\frac{1}{4}}z.$$

It will be useful to introduce the combination

$$\lambda = v - \tfrac{1}{2}r\theta. \tag{A 9}$$

The solution of (A 8) satisfying the boundary conditions yields

$$\tilde{u} = D(r)(1+br^2)^{-\frac{1}{4}}\,\mathrm{e}^{-\zeta}\sin\zeta, \tag{A 10a}$$

$$\tilde{v} = D(r)(1+br^2)^{-1}\,\mathrm{e}^{-\zeta}\cos\zeta, \tag{A 10b}$$

$$\tilde{\theta} = -2brD(r)(1+br^2)^{-1}\,\mathrm{e}^{-\zeta}\cos\zeta, \tag{A 10c}$$

where

$$D(r) = -\lambda_{\mathrm{c}} + \lambda_{\mathrm{B}}. \tag{A 11}$$

Additional terms of similar form but $O(u_{\mathrm{c}})$ which are contributed by the radial velocity boundary condition were neglected, since the equation of azimuthal momentum implies $u_{\mathrm{c}} \ll v_{\mathrm{c}}$.

The values at the edge of the boundary layer are obtained by setting $\zeta = 0$:

$$v_{\mathrm{c}} = V_{\mathrm{B}} - D(r)(1+br^2)^{-1}, \tag{A 12a}$$

$$\theta_{\mathrm{c}} = \Theta_{\mathrm{B}} + 2brD(r)(1+br^2)^{-1}, \tag{A 12b}$$

and depend on the boundary conditions and λ_{c}. By integration of (A 10a) from 0 to ∞ the value of the stream function at the edge of the boundary layer is

$$\tilde{\psi}_{\mathrm{c}} = 2\pi\rho r\int_0^{\delta_z}\tilde{u}\,\mathrm{d}z = \pi\rho r\left(\frac{E}{\rho}\right)^{\frac{1}{2}}(1+br^2)^{-\frac{3}{4}}D(r). \tag{A 13}$$

From (A 10), the equation of continuity (A 1) and the boundary conditions we obtain

$$w_{\mathrm{c}} = -\frac{1}{2}\left(\frac{E}{\rho}\right)^{\frac{1}{2}}(1+br^2)^{-\frac{3}{4}}\left[\frac{1}{2}\frac{D}{r}\left(-1+M^2r^2+\frac{3}{1+br^2}\right)+\frac{\mathrm{d}D}{\mathrm{d}r}\right]+W_{\mathrm{B}}. \tag{A 14}$$

Appendix B. The flow in the vertical $E^{\frac{1}{3}}$ shear layers at $r = r_1$

We denote by $\hat{(\ )}$ the linear corrections in this layer. The equations of motion are

$$\frac{\partial\hat{u}}{\partial r}+\frac{\partial\hat{w}}{\partial z}+M^2r_1\hat{u} = 0, \tag{B 1}$$

$$-2\hat{v}+r_1\hat{\theta} = -\frac{1}{M^2}\frac{\partial\hat{\alpha}}{\partial r}, \tag{B 2}$$

$$2\hat{u} = \frac{E}{\rho}\frac{\partial^2\hat{v}}{\partial r^2}, \tag{B 3}$$

$$0 = -\frac{1}{M^2}\frac{\partial\hat{\alpha}}{\partial z}+\frac{E}{\rho}\frac{\partial^2\hat{w}}{\partial r^2}, \tag{B 4}$$

$$-4br_1\hat{u} = \frac{E}{\rho}\frac{\partial^2\hat{\theta}}{\partial r^2}. \tag{B 5}$$

The relative changes of ρ in this layer are $O[\exp(M^2 r_1 \delta)]$, where $\delta = [HE/\rho(r_1)]^{\frac{1}{3}}$. For $\delta \ll M^{-2} r_1^{-1}$, $\rho(r)$ can be approximated by $\rho(r_1)$ in (B 3)–(B 5), and the last term in (B 1) can be neglected, resulting in a system similar to that treated by Hunter (1967). Otherwise, a more complicated treatment is required, as described by Bark & Bark (1976). For the sake of simplicity, let $\delta \ll M^{-2} r_1^{-1}$, and introduce the local incompressible stream function

$$\hat{u} = \frac{\partial \hat{\psi}}{\partial z}, \quad w = -\frac{\partial \hat{\psi}}{\partial r} \tag{B 6}$$

and the local Ekman number $E_1 = E/\rho(r_1)$. By elimination among (B 1)–(B 6), a single equation is obtained for $\hat{\psi}$:

$$\frac{\partial^6 \hat{\psi}}{\partial x^6} + \frac{4(1+br_1^2)}{E_1^2} \frac{\partial^2 \hat{\psi}}{\partial z^2} = 0, \tag{B 7}$$

where $x = |r - r_1|$.

Matching to the outer flow requires

$$\hat{\psi} \to 0, \quad \hat{v} \to 0, \quad \hat{\theta} \to 0 \quad \text{as } x \to \infty. \tag{B 8}$$

From (B 3), (B 5) and (B 8), we obtain

$$\frac{\hat{\theta}}{\hat{v}} = -2br_1, \tag{B 9}$$

therefore

$$\hat{\lambda} = \hat{v} - \tfrac{1}{2} r_1 \hat{\theta} = -\frac{1+br_1^2}{2br_1} \hat{\theta}.$$

Boundary conditions for (B 7) on $z = 0, H$ are obtained by matching with the Ekman boundary layers. Solutions of (B 7) satisfying the boundary condition are of the form

$$\hat{\psi} = C_1 \exp(-\xi x) + C_2 \exp(-\tfrac{1}{2}\xi x) \cos\left(\frac{\sqrt{3}}{2} \xi x + \phi\right) \sin \frac{\pi l}{H} z, \tag{B 10}$$

where

$$\xi = (1+br_1^2)^{\frac{1}{3}} \left(\frac{2\pi l}{E_1 H}\right)^{\frac{1}{3}}, \tag{B 11}$$

where l is an integer. C_1, C_2 and ϕ are (real) constants. Finally, we note that the orders of magnitude of the variables that satisfy the equations of motion are

$$\{\hat{u}, \hat{v}, \hat{w}, \hat{\theta}, \hat{\lambda}, \hat{\psi}\} = A \left\{\left(\frac{E_1}{H^2}\right)^{\frac{1}{3}}, 1, 1, 1, 1, (HE_1)^{\frac{1}{3}}\right\}. \tag{B 12}$$

The value of A is 1 for the layer required to match the boundary condition on λ (this layer also matches θ and v), and $E^{\frac{1}{3}} H^{-\frac{1}{3}}$ for the layer that matches and smoothes u and w. The former layer is required for the solution of λ in the extended core, and will be discussed in some detail below.

B.1. *Matching* λ

The boundary conditions at $r = r_b$ are

$$\hat{\lambda} + \lambda^o = V_b(z) - \tfrac{1}{2} r_b \Theta_b(z) \equiv \lambda_b(z), \tag{B 13a}$$

$$\hat{\psi} + \psi^o = 0, \tag{B 13b}$$

$$-\frac{\partial \hat{\psi}}{\partial r} + w^o = 0, \tag{B 13c}$$

$$\hat{\theta} + \theta^o = \Theta_b(z), \tag{B 13d}$$

where $(\ )^{\circ}$ is the corresponding 'outer' solution in the extended core. Equations (B 13a, d) imply the boundary conditions for the azimuthal velocity, namely $\hat{v}+v^{\circ} = V_{\mathrm{b}}(z)$. Here $V_{\mathrm{b}}(z)$ and $\Theta_{\mathrm{b}}(z)$ are the prescribed values of v and θ at $r = r_{\mathrm{b}}$, and $r_{\mathrm{b}} = 1$ or r_{I}.

In the outer region ψ° and w° are small compared with $\hat{\psi}$ and $\hat{w}$. Therefore (B 13b, c) require that, to leading order, $\hat{\psi}$ and $\partial\hat{\psi}/\partial r$ equal zero at $r = r_{\mathrm{b}}$. For the same reason, the leading term in $\hat{\psi}$ must vanish at $z = 0, H$. These facts establish the recirculating feature of the flow in this region. The solution satisfying the homogeneous boundary conditions is

$$\hat{\psi} = \sum_{n=1}^{\infty} A_n \sin\left(\frac{n\pi}{H}z\right)\left[\exp(-\delta_n x)-\frac{2}{\sqrt{3}}\exp(-\tfrac{1}{2}\delta_n x)\cos\left(\frac{\sqrt{3}}{2}\delta_n x+\tfrac{1}{6}\pi\right)\right], \tag{B 14}$$

$$\hat{\lambda} = (1+br_1^2)^{\frac{1}{2}}\sum_{n=1}^{\infty} A_n\delta_n\cos\left(\frac{n\pi}{H}z\right)\left[\exp(-\delta_n x)+\frac{2}{\sqrt{3}}\exp(-\tfrac{1}{2}\delta_n x)\cos\left(\frac{\sqrt{3}}{2}\delta_n x-\tfrac{1}{6}\pi\right)\right], \tag{B 15}$$

where $$\delta_n = \left(\frac{2n\pi}{E_1 H}\right)^{\frac{1}{3}}(1+br_1^2)^{\frac{1}{6}}.$$

Imposing the boundary conditions (B 13a, d) we obtain

$$\lambda^{\circ} = \frac{1}{H}\int_0^H \lambda_{\mathrm{b}}(z)\,\mathrm{d}z, \tag{B 16}$$

$$A_n = \frac{1}{H}\frac{1}{(1+br_1^2)^{\frac{1}{2}}}\frac{1}{\delta_n}\int_0^H \lambda_{\mathrm{b}}(z)\cos\left(n\pi\frac{z}{H}\right)\mathrm{d}z, \tag{B 17}$$

$$\theta^{\circ} = \Theta_{\mathrm{b}}(z)+\frac{2br_{\mathrm{b}}}{1+br_{\mathrm{b}}^2}[\lambda_{\mathrm{b}}(z)-\lambda^{\circ}]. \tag{B 18}$$

Equation (B 16) and (B 18) provide the boundary conditions for the solution of the extended core. In the present case the flow in this layer is completely defined by the boundary conditions on the outer wall. Therefore the matching condition with the outer flow (the extended core) is explicitly given in terms of these boundary conditions. When the outer wall is insulated, the decoupling of the $E^{\frac{1}{3}}$ layer from the inner flow is not possible, as pointed out by Homsy & Hudson (1969) and Matsuda & Takeda (1978).

B.2. *Matching u and w (the mass flux)*

These shear layers are also required for matching the boundary conditions $u = w = 0$ on the vertical walls and for smoothing u and w in regions of discontinuities of the horizontal boundary condition ('split disk', point source). These layers transport an $O(E^{\frac{1}{2}})$ mass flux from the Ekman layers and into the extended core; therefore they are often treated in connection with the matching of the mass flux. Consequently, $A = (E_1/H^2)^{\frac{1}{6}}$ in (B 12) gives the order of magnitude of the variables, and we can see that λ (and consequently θ and v) are not affected (to leading order) in these regions. Solutions of (B 7) for the flow field in these regions can be obtained as a straightforward extension of the solutions given by Greenspan (1969) and Hunter (1967).

REFERENCES

BARCILON, V. 1970 Some inertial modifications of the linear viscous theory of steady rotating fluid flows. *Phys. Fluids* **13**, 537–544.

BARCILON, V. & PEDLOSKY, J. 1967 Linear theory of rotating stratified fluid motions. *J. Fluid Mech.* **23**, 1–16.

BARK, F. H. & BARK, T. H. 1976 On vertical boundary layers in a rapidly rotating gas. *J. Fluid Mech.* **78**, 749–761.

BARK, F. H., MEIJER, P. S. & COHEN, H. I. 1978 Spin up of a rapidly rotating gas. *Phys. Fluids* **21**, 531–539.

BENNETTS, D. A. & HOCKING, L. M. 1973 On nonlinear Ekman and Stewartson layers in a rotating fluid. *Proc. R. Soc. Lond.* A **333**, 469–489.

CONLISK, A. T., FOSTER, M. R. & WALKER, J. D. A. 1982 Fluid dynamics and mass transfer in a gas centrifuge. *J. Fluid Mech.* **125**, 283–317.

DUNCAN, I. B. 1966 Axisymmetric convection between two rotating disks. *J. Fluid Mech.* **24**, 417–449.

GREENSPAN, H. P. 1969 *The Theory of Rotating Fluids.* Cambridge University Press.

HOMSY, G. M. & HUDSON, J. L. 1969 Centrifugally driven thermal convection in a rotating cylinder. *J. Fluid Mech.* **35**, 33–52.

HUDSON, J. L. 1968*a* Non isothermal flow between rotating disks. *Chem. Engng Sci.* **23**, 1007.

HUDSON, J. L. 1968*b* Convection near a cooled disk rotating with its environment. *Intl J. Heat Mass Transfer* **11**, 407.

HULTGREN, L. S. 1978 Stability of axisymmetric gas flows in a rapidly rotating cylindrical container. Ph.D. thesis, MIT.

HUNTER, C. 1967 The axisymmetric flow in a rotating annulus due to a horizontal applied temperature gradient. *J. Fluid Mech.* **27**, 753–778.

ISRAELI, M. & UNGARISH, M. 1981 Improvement of numerical schemes by incorporation of approximate solutions applied to rotating compressible flows. In *Proc. 7th Intl Conf. on Numerical Methods in Fluid Dynamics* (ed. W. C. Reynolds & R. W. MacCormack). Lecture Notes in Physics, vol. 141, pp. 230–235. Springer.

ISRAELI, M. & UNGARISH, M. 1983 Laminar compressible flow between close rotating disks – an asymptotic and numerical study. *Comp. Fluids* **11**, 145–157.

MATSUDA, T. & HASHIMOTO, K. 1978 The structure of the Stewartson layers in a gas centrifuge. Part 1. Insulated endplates. *J. Fluid Mech.* **85**, 433–442.

MATSUDA, T., SAKURAI, T. & TAKEDA, H. 1975 Source–sink flow in a gas centrifuge. *J. Fluid Mech.* **69**, 197–208.

MATSUDA, T. & TAKEDA, H. 1978 The structure of the Stewartson layers in a gas centrifuge. Part 2. Insulated side wall. *J. Fluid Mech.* **85**, 443–457.

MOORE, D. W. & SAFFMAN, P. G. 1969 The structure of free vertical layers in a rotating fluid and the motion produced by a slowly rising body. *Phil. Trans. R. Soc. Lond.* A **264**, 597–634.

RILEY, N. 1967 Thermally induced boundary-layer flows in a rotating environment. *J. Fluid Mech.* **29**, 241–257.

SAKURAI, T. & MATSUDA, T. 1974 Gasdynamics of a centrifugal machine. *J. Fluid Mech.* **62**, 727–736.

TOREN, M. 1976 Compressible isothermal flow over a stationary disk confined in a rotating cylindrical container. Ph.D. Thesis, Technion, Haifa, Israel.

TOREN, M. & SOLAN, A. 1979 Laminar compressible flow over a stationary disk in a rotating cylinder. *Trans. ASME* I: *J. Fluids Engng* **101**, 173–180.